

FULL PAPER

## Theoretical *ab initio* Study of $\text{TiCl}_4$ Ammonolysis: Gas Phase Reactions of TiN Chemical Vapor Deposition

Magdalena Siodmiak<sup>1</sup>, Gernot Frenking<sup>1</sup>, and Anatoli Korkin<sup>2</sup>

<sup>1</sup>Fachbereich Chemie, Philipps-Universität Marburg, Hans-Meerwein-Strasse, D-35032 Marburg, Germany.

<sup>2</sup>Advanced Systems Technology Lab, Motorola Inc., Mesa AZ 85202, USA. E-mail: r40757@email.sps.mot.com

Received: 11 November 1999/ Accepted: 18 January 2000/ Published: 28 April 2000

**Abstract** The mechanism of  $\text{TiCl}_4$  ammonolysis has been studied theoretically at *ab initio* Hartree-Fock, B3LYP, MP2 and CCSD(T)//B3LYP levels using effective core potentials for Ti and Cl and 6-31G\* basis sets for N and H.  $\text{TiCl}_4$  and products of its ammonolysis form five- and six-coordinated complexes with ammonia, which intermediate substitution of Cl atoms by  $\text{NH}_2$  groups. Transition state energies for the subsequent steps of ammonolysis decrease with increasing number of  $\text{NH}_2$  groups bound to Ti. The energy of the transition state for the first step of ammonolysis is 19 kcal mol<sup>-1</sup> above the energy of the reactants ( $\text{TiCl}_4 + \text{NH}_3$ ) and 8 kcal mol<sup>-1</sup> above the products ( $\text{TiCl}_3\text{NH}_2 + \text{HCl}$ ). The following steps have transition states energetically located below the products, indicating weak hydrogen bonded complex formation as intermediate between transition state and product. A thermodynamic estimation shows the last step of ammonolysis to be endothermic, while the first three steps are exothermic if the adduct formation energy is taken into account.

**Keywords** Titanium nitride, *Ab initio* calculations, Chemical vapor deposition, Ammonolysis, Donor-acceptor complexes

### Introduction

Titanium nitride has a unique combination of useful properties (high hardness and melting point, good electric and thermal conductivity, chemical inertness, and excellent adherence to most metals, semiconductors and insulators) and numerous existing and potential industrial applications. It has

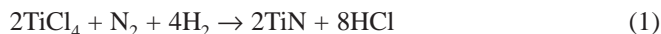
even been called as “technologically the most important nitride” [1] In microelectronics TiN has a broad area of applications as a low resistance contact and a diffusion barrier for metallization.[2]

Chemical vapor deposition (CVD) usually provides high quality film and good step coverage, and it is often superior to physical vapor deposition (PVD). Several precursors such as  $\text{TiCl}_4$ , [1,3]  $\text{Ti}(\text{NMe}_2)_4$ , [1,4,5]  $\text{Ti}(\text{NEt}_2)_4$  [1,4,6] and  $\text{Ti}(\text{NMeEt})_4$  [7] have been applied in titanium nitride deposition. The reaction of  $\text{TiCl}_4$  with  $\text{N}_2$  and  $\text{H}_2$  (eq. 1) has been used at first for TiN deposition at high (~900-1200°C) temperatures. The application of ammonia as a source of nitrogen (eq. 2) lowers the temperature to ~500°C, [3] which opens this process for a broader application in the micro-

Correspondence to: A. Korkin

Dedicated to Professor Paul von Ragué Schleyer on the occasion of his 70<sup>th</sup> birthday

electronics industry. Organometallic precursors such as  $\text{Ti}(\text{NR}_2)_4$  contain an excess of nitrogen. However, simple thermal decomposition leads to a high carbon contamination, while addition of ammonia improves the film composition and also lowers the process temperature.



The optimization of the CVD conditions for obtaining higher quality films, better conformity or higher (optimal) film growth rate requires knowledge of the deposition chemistry, which can be obtained from specially designed experiments or/and modeling and simulation. Recent developments of quantum chemical methods, particularly density functional theory (DFT), and software and fast progress in computational hardware have provided first principles (*ab initio*) based theoretical quantum chemistry approaches as an alternative to experiments and empirical simulations in some areas of CVD modeling. However, such studies still have serious limitations in the size of the system, and thus can be applied most efficiently only for smaller precursors and gas phase reactions. In our theoretical study we have considered initial reactions between  $\text{TiCl}_4$  and  $\text{NH}_3$  in order to provide some insight into the thermochemistry, mechanism and kinetics of CVD.

During the CVD process three types of (subsequent) processes occur. At lower temperatures  $\text{TiCl}_4$  and ammonia form donor-acceptor complexes, presumably with one or two ammonia, e.g.  $\text{TiCl}_4 \cdot \text{NH}_3$  and  $\text{TiCl}_4 \cdot 2\text{NH}_3$ . Fast complexation is followed by slow ammonolysis. At high temperatures Ti(IV) is reduced to Ti(III) in the form of  $\text{TiN}_x$  film or as a powder. These types of processes (e.g., complex formation, ammonolysis and reduction) are well known in the gas phase and solution chemistry of  $\text{TiCl}_4$  while their detailed mechanistic description is far from being well understood [8]. In liquid ammonia up to three chlorine atoms are substituted by  $\text{NH}_2$  groups, while in methylamine only two TiCl bonds are ammonolysed. Trimethylamine reduces Ti (IV) to Ti(III) and forms a complex with resulting titanium trichloride –  $\text{TiCl}_3 \cdot 2\text{NH}_3$ . Saeki et al. [9] observed  $\text{TiCl}_4 \cdot 5\text{NH}_3$  as a product of the gas phase reaction between  $\text{TiCl}_4$  and  $\text{NH}_3$  at a temperature below  $220^\circ\text{C}$ , which presumably consists of a mixture of  $\text{NH}_4\text{Cl}$  with an ammonia adduct of the partially aminolyzed  $\text{TiCl}_4$ . In the temperature range between  $220^\circ\text{C}$  and  $430^\circ\text{C}$   $\text{TiCl}_4 \cdot 5\text{NH}_3$  decomposes to  $\text{ClTiN}$ , which at higher temperatures reacts with ammonia forming  $\text{TiN}_x$  powder [9]. The thermochemistry of gas-phase species relevant to TiN CVD has been studied theoretically by Allendorf et al. [10] who reported a  $17 \text{ kcal mol}^{-1}$  exothermic enthalpy of the 1:1 complex formation between  $\text{TiCl}_4$  and  $\text{NH}_3$  and a  $20 \text{ kcal mol}^{-1}$  endothermic decomposition energy of this complex toward  $\text{Cl}_3\text{TiNH}_2$  and  $\text{HCl}$ . Ti-C and Ti-N bond energies have been also reported in ref. [10]. It was found that the Ti-Cl bond energies computed at CCSD(T) and at BLYP levels are in good agreement with each other. Structures and energetics of some intermediates in TiN CVD:  $\text{TiCl}_m(\text{NH}_2)_n$ ,

$\text{TiCl}_m(\text{NH}_2)_n\text{NH}$  and  $\text{TiCl}_m(\text{NH}_2)_n\text{N}$  have been calculated by Schlegel et al [11] using a variant of G2 level theory.

In this paper we have studied theoretically subsequent steps of  $\text{TiCl}_4$  ammonolysis and 1:1 and 1:2 complexes of  $\text{TiCl}_4 \cdot (\text{NH}_2)_x$  ( $x = 1-4$ ) molecules with ammonia using different *ab initio* (HF, MP2, CCSD(T)) and DFT (B3LYP) methods in combination with pseudopotentials for Ti and Cl atoms. The study has been done as a part of a joint project between the Philipps University Marburg and Motorola in the aim of developing a mechanism of TiN chemical vapor deposition.

---

## Computational methods

Molecular geometries have been optimized using three different theoretical methods: HF, MP2 [12] and B3LYP [13] as implemented in the Gaussian98 program package [14]. Analytical harmonic frequencies have been computed at the HF level of theory for all stationary structures and at the B3LYP and MP2 levels for selected molecules. HF vibrational frequencies are scaled by 0.89 [15]. Using B3LYP optimized geometries single point coupled cluster CCSD(T) [16] calculations have been performed<sup>17</sup>. The relative energies presented in this paper include zero-point energy (ZPE) corrections.

All calculations were performed using a quasi-relativistic effective core potential (ECP) for titanium with a valence basis set (441/2111/41), derived [18] from the [55/5/5] valence basis set of Hay and Wadt [19]. An ECP with a valence basis set (4/5)/[2s3p] [20] extended by a *d*-type polarization function [21] was used for chlorine. It has been demonstrated for a representative set of transition metal complexes [22] that ECP's generated for *ab initio* methods can be applied in DFT-based calculations as well. Standard 6-31G\* basis sets [23] were used for nitrogen and hydrogen atoms. Unless specified otherwise, relative energies are given at the CCSD(T)//B3LYP level and the structural parameters for the B3LYP optimized geometries.

---

## Results and discussion

Titanium tetrachloride reacts with gaseous or liquid ammonia by forming adducts, which are further ammonolyzed in excess of ammonia [24]. When  $\text{TiCl}_4$  and  $\text{NH}_3$  are mixed at temperatures below 530K, also six-coordinated complexes with ammonia are observed [25], [26]. In our paper we have considered first the following four-coordinated molecules:  $\text{TiCl}_4$ ,  $\text{TiCl}_3\text{NH}_2$ ,  $\text{TiCl}_2(\text{NH}_2)_2$ ,  $\text{TiCl}(\text{NH}_2)_3$  and  $\text{Ti}(\text{NH}_2)_4$  and their 1:1 and 1:2 complexes with ammonia.

### Four-coordinated titanium containing molecules

The optimized geometries of  $\text{TiCl}_4$ ,  $\text{TiCl}_3\text{NH}_2$ ,  $\text{TiCl}_2(\text{NH}_2)_2$ ,  $\text{TiCl}(\text{NH}_2)_3$  and  $\text{Ti}(\text{NH}_2)_4$  at B3LYP, HF and MP2 level are

shown in Figure 1. Experimental structures and vibrational frequencies are available only for  $\text{TiCl}_4$  [27] (Table 1). The Ti-Cl bond length determined by gas electron diffraction is 2.170 Å. Thus, all three methods, HF, MP2 and B3LYP, are within 0.01 Å of the Ti-Cl bond length (see Figure 1a). B3LYP gives a larger and HF and MP2 a smaller value compared with the experimental results. In earlier HF all electron [28], HF pseudopotential [29] and local density functional studies, [30] the Ti-Cl bond length in  $\text{TiCl}_4$  was computed as 2.165 Å, 2.184 Å and 2.167 Å, respectively.

The calculated HF vibrational frequencies are in a good agreement with experimental values [26] and previous theo-

retical studies using HF ECP [28] and LDF [29] approaches (see Table 1). The vibrational modes computed at the B3LYP and at the MP2 approaches are higher than the experimental values.

Consecutive substitution of Cl by  $\text{NH}_2$  in the  $\text{TiCl}_{4-x}(\text{NH}_2)_x$  ( $x = 0-4$ ) series leads to elongation of both Ti-Cl and Ti-N bond lengths. Thus the first two molecules in the series,  $\text{TiCl}_4$  and  $\text{TiCl}_3(\text{NH}_2)$ , have the shortest Ti-Cl (2.176 Å) and Ti-N (1.855 Å) bond lengths, respectively, while the last two,  $\text{TiCl}(\text{NH}_2)_3$  (Ti-Cl = 2.259 Å and  $\text{Ti}(\text{NH}_2)_4$ , (Ti-N = 1.912 Å) have the longest ones. An earlier RHF ECP [31] study of  $\text{TiClH}_2(\text{NH}_2)$  and  $\text{TiH}_2(\text{NH}_2)_2$  predicts Ti-N bonds to be 1.86

**Figure 1** B3LYP optimized geometries of four coordinated titanium compounds: a)  $\text{TiCl}_4$ , b)  $\text{TiCl}_3\text{NH}_2$ , c)  $\text{TiCl}_2(\text{NH}_2)_2$ , d)  $\text{TiCl}(\text{NH}_2)_3$ , e)  $\text{Ti}(\text{NH}_2)_4$ . HF and MP2 values are given in parentheses

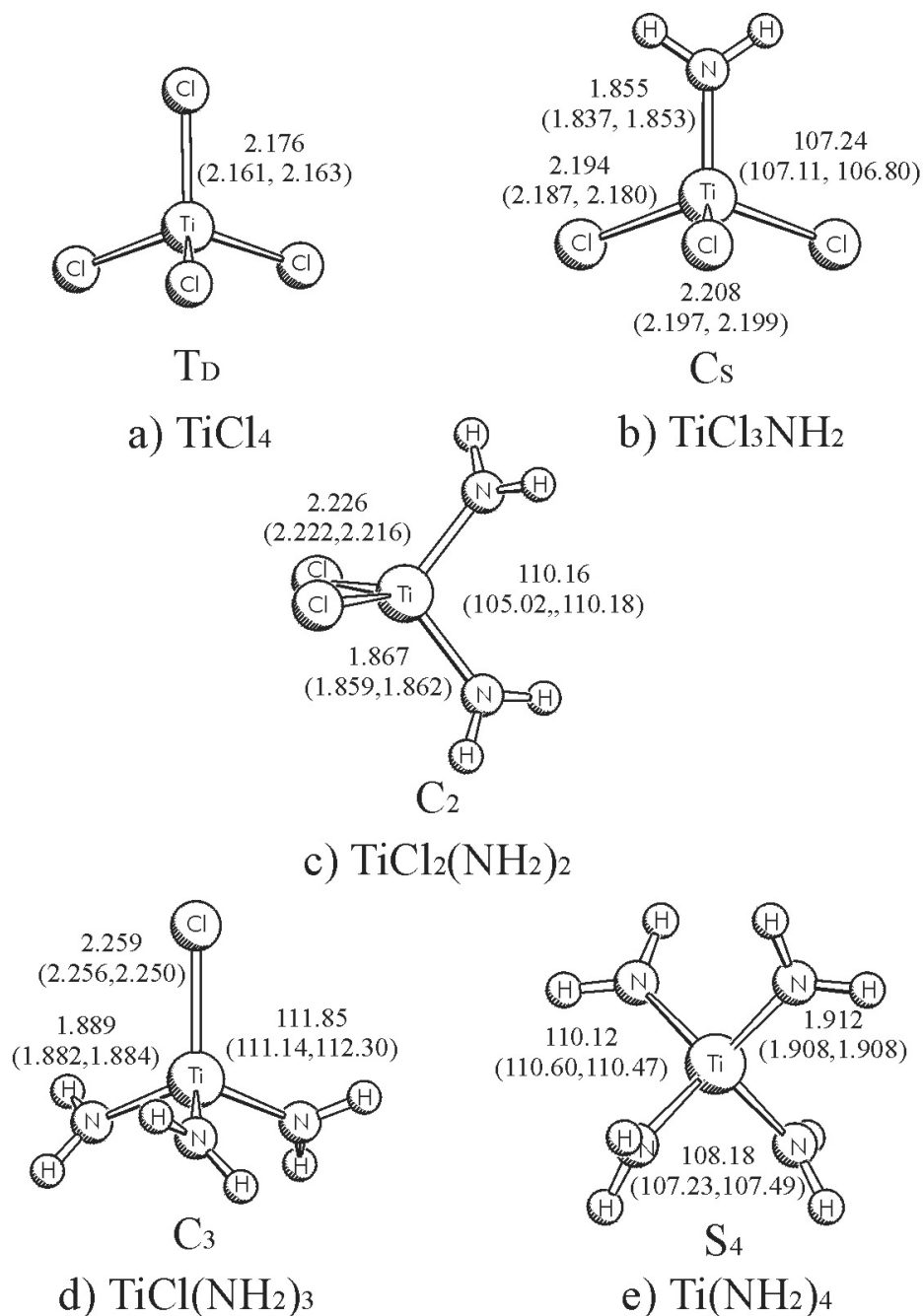


**Table 1** Computed and experimental vibrational frequencies (in  $\text{cm}^{-1}$ ) for  $\text{TiCl}_4$ 

[a] from ref. 27  
 [b] from ref. 28  
 [c] from ref. 25

	HF	B3LYP	MP2	Calc. [a]	Calc. [b]	Exp. [c]
$\nu_1(\text{a}_1)$	389	397	407	403	377	388
$\nu_2(\text{e})$	112	121	122	117	96	118
$\nu_3(\text{t}_2)$	484	514	533	518	507	497
$\nu_4(\text{t}_2)$	138	144	141	144	129	139

**Table 2** Complex formation energies ( $\Delta H_c$ ) (in  $\text{kcal mol}^{-1}$ ) for  $\text{TiCl}_{4-x}(\text{NH}_2)_x:\text{yNH}_3$  ( $x=0-4$ ;  $y=1-2$ ) adducts [a]

$\text{TiCl}_{4-x}(\text{NH}_2)_x:\text{yNH}_3$		HF	B3LYP	MP2	CCSD(T)
$\text{TiCl}_4$	1:1	18.3	18.3	23.6	23.6
	1:2	35.9 (35.8) [b]	34.7 (32.9) [b]	47.4 (43.8) [b]	47.4 (44.9) [b]
$\text{TiCl}_3\text{NH}_2$	1:1	17.1	17.5	23.3	23.2
	1:2	34.7	33.6	46.9	46.8
$\text{TiCl}_2(\text{NH}_2)_2$	1:1	13.9	13.7	19.5	19.5
	1:2	27.9	28.0	40.4	40.5
$\text{TiCl}(\text{NH}_2)_3$	1:1	12.0	10.9	16.2	16.1
	1:2	19.9	17.7	33.1	29.5
$\text{Ti}(\text{NH}_2)_4$	1:1	7.2	7.9	12.8	13.3
	1:2	6.6	7.5	16.6	17.2

[a] Most stable conformations of complexes are considered. See text for details

[b] The  $\Delta H_c$  values for the trans conformations are given in parenthesis

Å and 1.89 Å, respectively. This is in good agreement with 1.855 Å and 1.867 Å obtained in our work for the Ti-N bonds in  $\text{TiCl}_3(\text{NH}_2)$  and  $\text{TiCl}_2(\text{NH}_2)_2$ , respectively. Experimental geometries for these compounds are not available. However, theoretical values of the TiN bond length in  $\text{Ti}(\text{NH}_2)_4$  (1.912 Å) and in  $\text{TiCl}(\text{NH}_2)_3$  (1.855 Å) are in good agreement with experimental data in the substituted compounds  $\text{Ti}(\text{NMe}_2)_4$  (1.917 Å) [32] and  $\text{Cl}_3\text{TiCl}_3\text{NEt}_2$  (1.852 Å) [33].

Amino groups attached to Ti in the calculated molecules are planar, which indicates a delocalization of the nitrogen lone pairs towards the empty *d*-orbitals of titanium.

#### Five-coordinated complexes

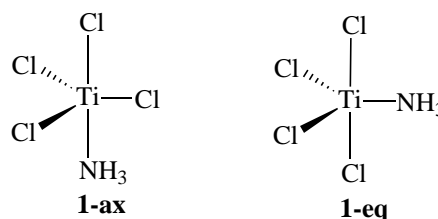
Tetracoordinated titanium molecules  $\text{TiCl}_{4-x}(\text{NH}_2)_x$  form relatively strong donor-acceptor complexes with ammonia. The energy of the  $\text{TiCl}_4:\text{NH}_3$  complex formation ( $\Delta H_c$ ) (see Table 2) varies from 18.3  $\text{kcal mol}^{-1}$  (HF and BL3LYP) to 23.6  $\text{kcal mol}^{-1}$  (MP2 and CCSD(T)), which can be compared with previous theoretical values of 24.3 and 17  $\text{kcal mol}^{-1}$  calculated using MP2 ECP [34] and BLYP [10] methods, respectively.

The complexes of  $\text{TiCl}_x(\text{NH}_2)_{4-x}$  with ammonia have bipyramidal structures. For the  $\text{TiCl}_4:\text{NH}_3$  complex two conformations (geometric isomers)<sup>35</sup> are visualized with  $\text{NH}_3$  occupying the axial or equatorial positions in Scheme 1.

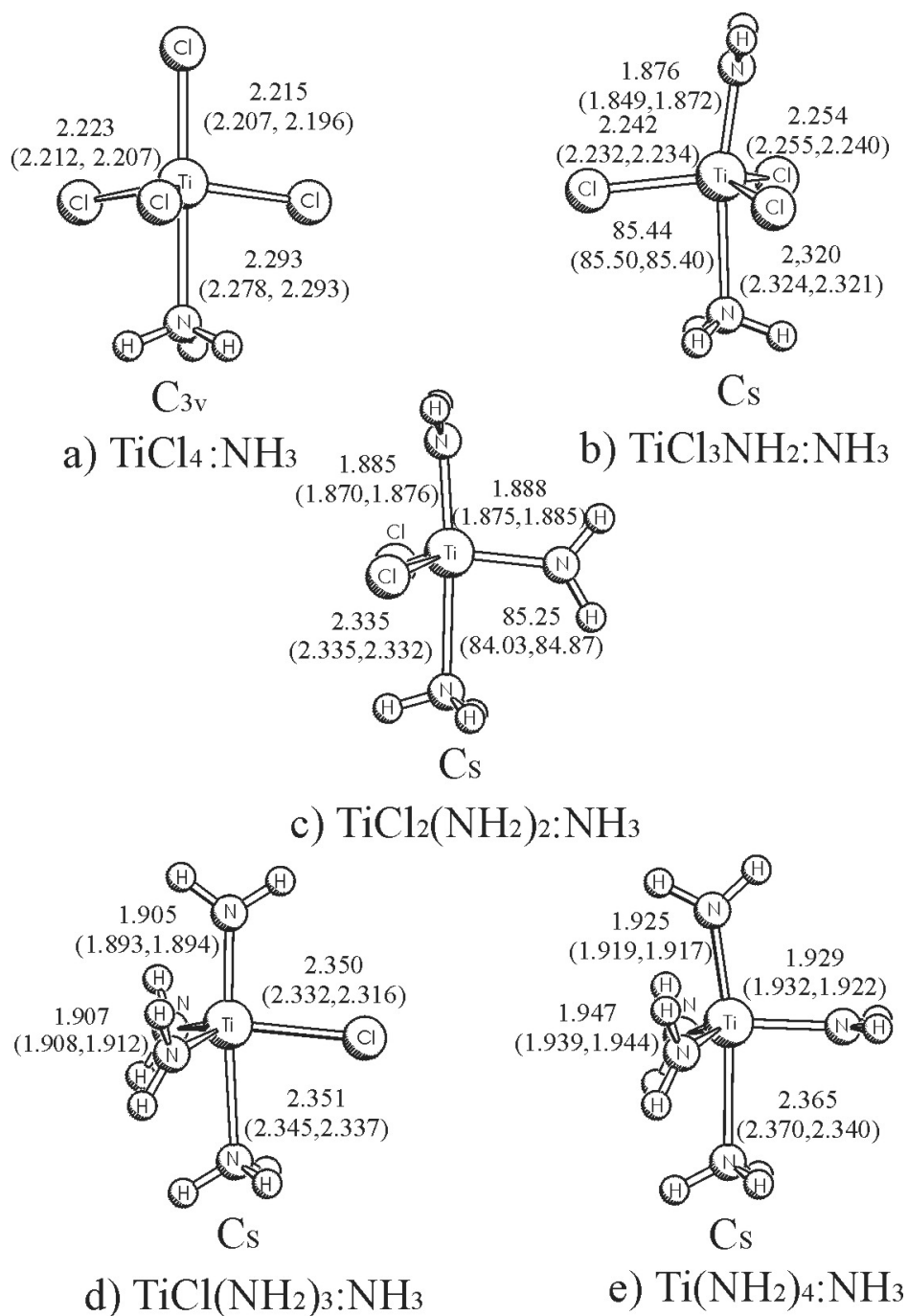
Structure **1-eq** collapses into **1-ax** during optimization at the B3LYP level and has thus not been investigated further. The Ti-Cl bond length for of axial chlorine atom in **1-ax** (see also Figure 2a) is shorter compared to the equatorial ones, which is unusual for bipyramidal structures [36]. An elongation of the equatorial bonds in **1-ax** can be explained by hydrogen bonding between equatorial chlorine atoms and the hydrogen atoms of ammonia. We have previously observed a similar effect in pentacoordinated oxichlorides  $\text{TaCl}_4(\text{OH})$  and  $\text{TaCl}_3(\text{OH})_2$  [37].

Four possible conformations with regard to axial and equatorial orientation are visualized for the  $\text{TiCl}_3\text{NH}_2:\text{NH}_3$  complex in Scheme 2.

All methods except HF predict the **2-ax,ax** conformation ( $\text{NH}_2$  and  $\text{NH}_3$  in axial positions) to be the most stable one.

**Scheme 1** Possible conformers of  $\text{TiCl}_4:\text{NH}_3$

**Figure 2** B3LYP optimized geometries of five coordinated titanium complexes with ammonia: (a)  $\text{TiCl}_4\text{-NH}_3$ , (b)  $\text{TiCl}_3\text{NH}_2\text{-NH}_3$ , (c)  $\text{TiCl}_2(\text{NH}_2)_2\text{-NH}_3$ , (d)  $\text{TiCl}(\text{NH}_2)_3\text{-NH}_3$ , (e)  $\text{Ti}(\text{NH}_2)_4\text{-NH}_3$ . HF and MP2 values are given in parentheses



The energy difference is small ( $\sim 1 \text{ kcal mol}^{-1}$ ) at all four theory levels considered (see Table 3). The **2-*eq,ax*** conformer collapses into **2-*ax,eq*** during optimization at the B3LYP level and was thus not considered further. The Ti-Cl and Ti-NH<sub>3</sub> bond lengths in **2-*ax,ax*** are elongated compared to **1-*ax*** (see Figures 2a and 2b). Thus, similar to the tetracoordinated molecules, substitution of Cl by NH<sub>2</sub> leads to elongation of *all* bonds in their complexes with ammonia. This effect is apparent in other NH<sub>3</sub> complexes discussed below. The  $\Delta H_c$  value of the most stable  $\text{TiCl}_3\text{NH}_2\text{:NH}_3$  conformer, **2-*ax,ax***, is very similar to that one of  $\text{TiCl}_4\text{:NH}_3$  (see Table 2). As well

as for  $\text{TiCl}_4\text{:NH}_3$ , the complex formation energies for  $\text{TiCl}_3\text{NH}_2\text{:NH}_3$  appear to be higher at MP2 and CCSD(T) compared to the values computed with the HF and the B3LYP approaches.

$\text{TiCl}_2(\text{NH}_2)_2\text{:NH}_3$  has five possible arrangements of the ligands with regard to their positions in a bipyramidal structure (Scheme 3).

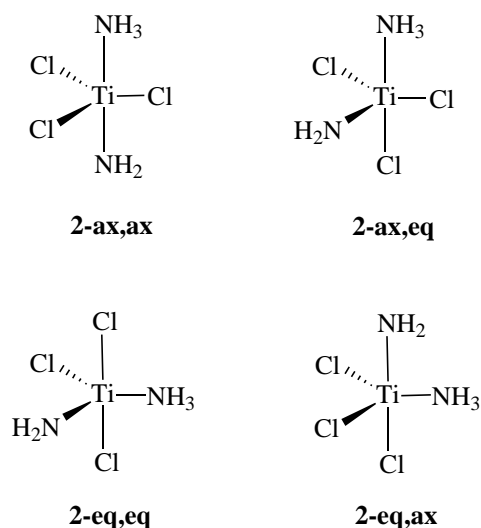
Similar to the  $\text{TiCl}_3\text{NH}_2\text{:NH}_3$  complex, the **3-*ax,ax,eq*** conformer of  $\text{TiCl}_2(\text{NH}_2)_2\text{:NH}_3$  with NH<sub>2</sub> and NH<sub>3</sub> ligands in the axial positions has been found to be most stable at the B3LYP level. Somewhat unexpectedly, another conformation

**Table 3** Relative energies of  $TiCl_3NH_2:NH_3$  conformers in  $kcal\ mol^{-1}$  (see Scheme 2)

	HF	B3LYP	MP2	CCSD(T)
2-ax,ax	0.0	0.0	0.0	0.0
2-ax,eq	-0.2	1.2	1.0	0.8
2-eq,eq	2.8	2.6	3.1	3.3
2-eq,ax	– Collapses into 2-ax,eq –			

with an axial position of ammonia, **3-ax,eq,eq**, was found to be slightly higher in energy compared to **3-eq,eq,eq**, where all nitrogens are located in the equatorial positions. Two other conformations **3-eq,ax,eq** and **3-eq,ax,ax** collapsed to **3-ax,eq,eq** and to **3-eq,eq,eq**, respectively. We also computed the most stable conformation, **3-ax,ax,eq** at the HF, MP2 and CCSD(T)//B3LYP levels of theory (see Figure 2c).

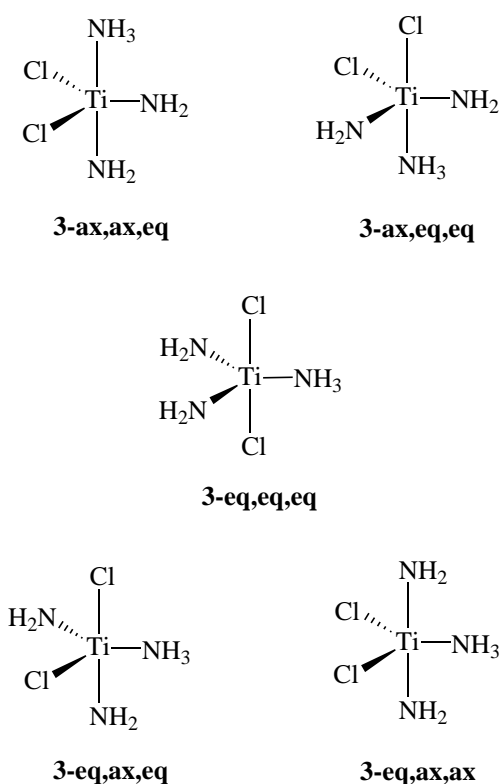
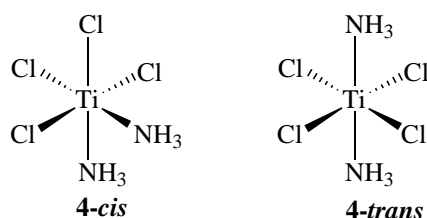
While the complex formation energies are close for  $TiCl_4$  and  $TiCl_3NH_2$ , the following steps of the ammonolysis reduce  $\Delta H_c$  by 3-4  $kcal\ mol^{-1}$  (see Table 2). The drop in  $\Delta H_c$  at the second and subsequent steps of the ammonolysis can be explained as follows. The first substitution of Cl by  $NH_2$  takes place in an axial position, while in further steps the Cl atoms are replaced in the equatorial positions. Completely ammonolyzed  $Ti(NH_2)_4$  forms a 1:1 adduct with  $NH_3$  with an energy of only 13.3  $kcal\ mol^{-1}$ , which is about half the  $\Delta H_c$  value of  $TiCl_4:NH_3$ . Although  $TiCl(NH_2)_3:NH_3$  may have four conformations with different orientation of the ligands in the bipyramidal structure, we limited ourselves by computing only the isomer with axial positions of  $NH_2$  and  $NH_3$  (see Figure 2d) which is expected to be the lowest one according to conformational studies of  $TiCl_3NH_2:NH_3$  and  $TiCl_2(NH_2)_2:NH_3$ . For the  $Ti(NH_2)_4:NH_3$  complex we computed the conformation with an axial orientation of ammonia (see Figure 2e).

**Scheme 2** Possible conformations of  $TiCl_3NH_2:NH_3$ 

## Six-coordinated complexes

Titanium tetrachloride forms a six-coordinated adduct with the second  $NH_3$  molecule with almost the same Ti- $NH_3$  bond strength as the first one (see Table 2). There are two possible  $TiCl_4:2NH_3$  conformers, e.g. with *cis* and *trans* orientation of  $NH_3$  in the tetragonal bipyramidal structure of the complex (Scheme 4).

Both conformers have almost the same energy at the HF level, while the correlated methods show the **4-cis** form to be 2-3  $kcal\ mol^{-1}$  more stable compared to **4-trans** (Table 2). The relatively small energy difference between the *cis* and *trans* forms of  $TiCl_4:2NH_3$  can be explained by a balance of van der Waals repulsion of ligands (larger in the **4-cis** conformer) and the  $TiCl_4$  deformation energy (larger in the **4-trans** conformer) (see Figures 3a and 3b). Four other 1:2 com-

**Scheme 3** Possible arrangements of  $TiCl_2(NH_2)_2:NH_3$ **Scheme 4** *cis* and *trans* conformers of  $TiCl_4:2NH_3$

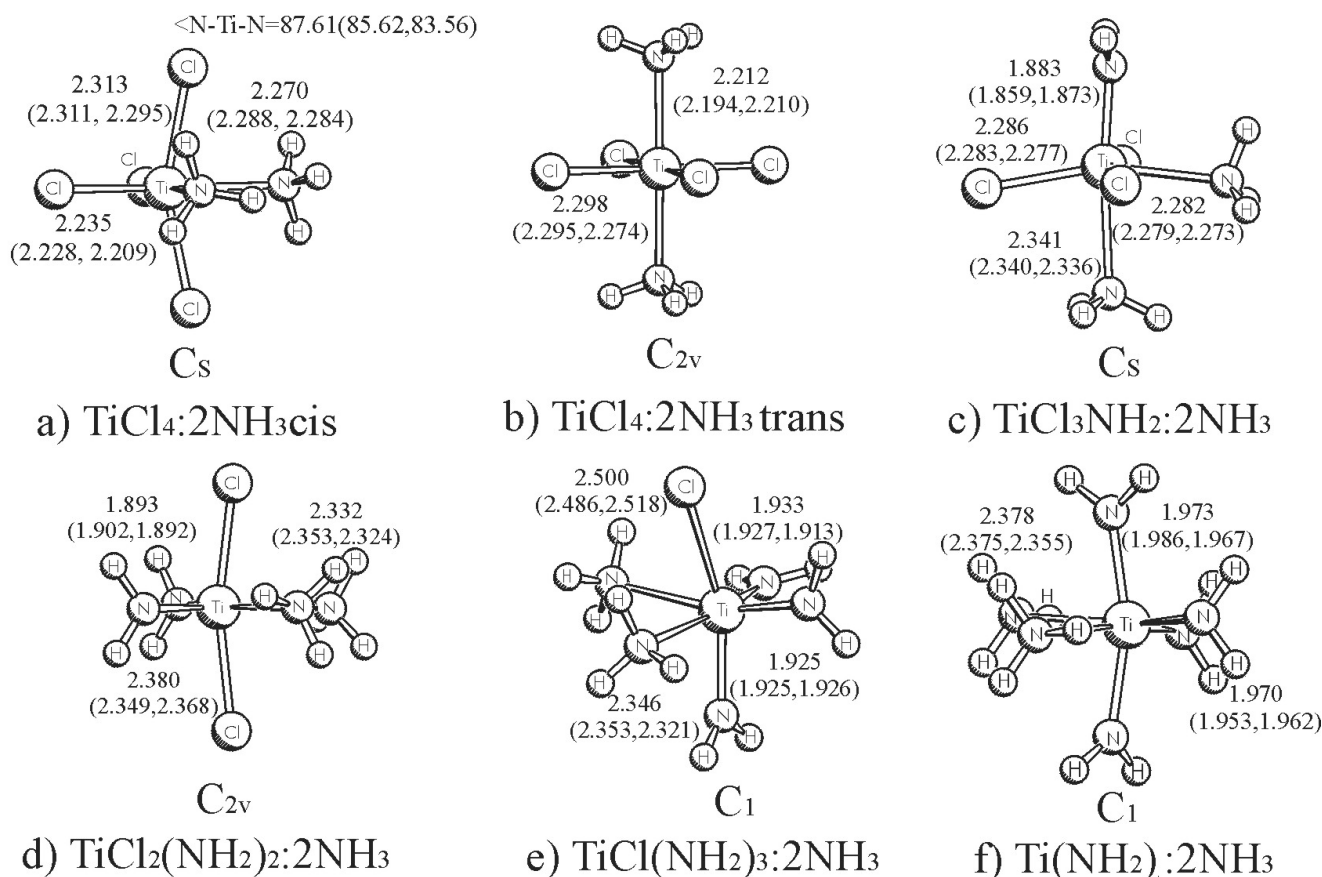


**Figure 3** B3LYP optimized geometries of six coordinated titanium complexes with two ammonia molecules: (a)  $\text{TiCl}_4:2\text{NH}_3$ , (b)  $\text{TiCl}_3\text{NH}_2:2\text{NH}_3$ , (c)  $\text{TiCl}_2(\text{NH}_2)_2:2\text{NH}_3$ , (d)

$\text{TiCl}(\text{NH}_2)_3:2\text{NH}_3$ , (e)  $\text{Ti}(\text{NH}_2)_4:2\text{NH}_3$ . HF and MP2 values are given in parentheses

plexes have been computed only for the *cis* conformation of two  $\text{NH}_3$  coordinated to Ti (see Figure 3c-f).

Substitution of chlorine atoms by  $\text{NH}_2$  in  $\text{TiCl}_x(\text{NH}_2)_{4-x}:2\text{NH}_3$  leads (as in the case of the four-coordinated molecules and the corresponding 1:1 complexes) to elongation of the Ti-Cl and Ti-N bonds. A comparison of the TiCl and TiN bonds in the four-, five-, and six-coordinated complexes reveals an additional effect of elongation of both bonds when the coordination number of Ti increases through formation of dative Ti-NH<sub>3</sub> bonds.

Similar to 1:1 complexes,  $\Delta H_c$  values of the 1:2 complexes of  $\text{TiCl}_4$  and  $\text{TiCl}_3\text{NH}_2$  with ammonia are close to each other. The value of  $\Delta H_c$  drops again with further increase of the number of  $\text{NH}_2$  groups in the complexes (see Table 2). Note, that the  $\Delta H_c$  values of the 1:2 complexes are approximately twice as large as the energies of the 1:1 adducts, except for  $\text{Ti}(\text{NH}_2)_4$ . In the latter case the formation of the second Ti←NH<sub>3</sub> donor-acceptor bond is accompanied by a smaller energy release than the first one.

The results of an NBO analysis performed at the B3LYP level is shown in Table 4. The positive charge at Ti increases along with increasing number of  $\text{NH}_2$  groups in four-coordinated molecules and in 1:1 and 1:2 complexes. Thus, the elec-

trostatic component in the dative Ti←NH<sub>3</sub> bond should *increase* when the number of the  $\text{NH}_2$  groups increases. However, electrostatic repulsion between the ligands leads to the *decrease* of  $\Delta H_c$  with increasing number of  $\text{NH}_2$  groups in the molecule. Complexation by ammonia reduces the positive charge at the central atom, in agreement with dative character of the Ti←NH<sub>3</sub> bond.

#### Thermochemistry and mechanism of ammonolysis.

Substitution of the Cl atoms by  $\text{NH}_2$  groups is endothermic, and the heat of reaction increases with the number of amino groups in the molecule (see Table 5). Since substitution of Cl by  $\text{NH}_2$  reduces the binding energy in the complexes with ammonia, ammonolysis of the complexes is more endothermic than similar reactions of four-coordinated molecules. It is well known that an excess of ammonia replaces up to three Cl atoms while full ammonolysis does not occur [23]. This holds for gas phase reactions of  $\text{TiCl}_4$  and  $\text{NH}_3$  and for the reactions of  $\text{TiCl}_4$  with liquid  $\text{NH}_3$ . Since the reaction of  $\text{TiCl}_4$  with  $\text{NH}_3$  consists of two steps, *exothermic* complex formation (presumably with two ammonia) and *endothermic* sub-

**Table 4** B3LYP NBO charges ( $q$ ) at Ti atom in calculated complexes

	TiCl <sub>x</sub> (NH <sub>2</sub> ) <sub>4-x</sub>	TiCl <sub>x</sub> (NH <sub>2</sub> ) <sub>4-x</sub> :NH <sub>3</sub>	TiCl <sub>x</sub> (NH <sub>2</sub> ) <sub>4-x</sub> :2NH <sub>3</sub>
TiCl <sub>4</sub>	0.67	0.61	0.50
TiCl <sub>3</sub> NH <sub>2</sub>	0.92	0.84	0.74
TiCl <sub>2</sub> (NH <sub>2</sub> ) <sub>2</sub>	1.12	1.06	0.97
TiCl(NH <sub>2</sub> ) <sub>3</sub>	1.30	1.25	1.19
Ti(NH <sub>2</sub> ) <sub>4</sub>	1.46	1.33	1.25

**Table 5** Zero Kelvin heats of the subsequent steps of ammonolysis of TiCl<sub>4-x</sub>(NH<sub>2</sub>)<sub>x</sub> molecules and their 1:1 and 1:2 complexes with ammonia (in kcal mol<sup>-1</sup>)

Reaction	x=	HF	B3LYP	MP2	CCSD(T)
TiCl <sub>4-x</sub> :xNH <sub>3</sub> + NH <sub>3</sub> → TiCl <sub>3-x</sub> NH <sub>2</sub> :xNH <sub>3</sub> + HCl	0	9.2	10.5	12.1	10.8
	1	12.3	13.2	14.2	13.0
	2	10.5	11.7	12.5	11.4
TiCl <sub>3</sub> NH <sub>2</sub> :xNH <sub>3</sub> + NH <sub>3</sub> → TiCl <sub>2</sub> (NH <sub>2</sub> ) <sub>2</sub> :xNH <sub>3</sub> + HCl	0	13.4	13.2	14.9	13.5
	1	16.6	17.0	18.7	17.2
	2	20.2	18.8	21.4	19.7
TiCl <sub>2</sub> (NH <sub>2</sub> ) <sub>2</sub> :xNH <sub>3</sub> + NH <sub>3</sub> → TiCl(NH <sub>2</sub> ) <sub>3</sub> :xNH <sub>3</sub> + HCl	0	20.0	19.2	21.2	19.7
	1	21.9	22.0	24.6	23.1
	2	28.0	29.5	28.5	30.7
TiCl(NH <sub>2</sub> ) <sub>3</sub> :xNH <sub>3</sub> + NH <sub>3</sub> → Ti(NH <sub>2</sub> ) <sub>4</sub> :xNH <sub>3</sub> + HCl	0	25.6	25.2	27.8	26.0
	1	30.4	28.3	31.1	28.8
	2	38.9	35.3	44.3	38.3

**Table 6** Zero Kelvin heats of the subsequent stages of aminolysis of TiCl<sub>4</sub> accompanied by 1:2 complex formation with ammonia (in kcal mol<sup>-1</sup>) [a]

Reaction	HF	B3LYP	MP2	CCSD(T)
TiCl <sub>4</sub> + 4NH <sub>3</sub> → TiCl <sub>3</sub> NH <sub>2</sub> :2NH <sub>3</sub> + NH <sub>3</sub> :HCl	-36.5	-34.1	-45.8	-47.0
TiCl <sub>4</sub> + 6NH <sub>3</sub> → TiCl <sub>2</sub> (NH <sub>2</sub> ) <sub>2</sub> :2NH <sub>3</sub> + 2NH <sub>3</sub> :HCl	-27.3	-26.3	-35.5	-38.3
TiCl <sub>4</sub> + 8NH <sub>3</sub> → TiCl(NH <sub>2</sub> ) <sub>3</sub> :2NH <sub>3</sub> + 3NH <sub>3</sub> :HCl	-10.3	-7.8	-17.9	-18.6
TiCl <sub>4</sub> + 10NH <sub>3</sub> → Ti(NH <sub>2</sub> ) <sub>4</sub> :2NH <sub>3</sub> + 4NH <sub>3</sub> :HCl	17.6	16.6	15.4	8.8

[a] 11 kcal mol<sup>-1</sup> exothermic energy of NH<sub>3</sub>:HCl adduct formation computed in ref. [36a] has been uniformly added to all reaction energies

stitution of Cl by NH<sub>2</sub> groups, we calculated the overall reaction energies for the different stages of ammonolysis (see Table 6). We have also considered an exothermic effect of formation of an H-bonded adduct of NH<sub>3</sub> and HCl (10–11 kcal mol<sup>-1</sup>) [38]. With such approximations, a substitution of up to three Cl atoms by NH<sub>2</sub> groups appears to be exothermic, while the complete ammonolysis of TiCl<sub>4</sub> into Ti(NH<sub>2</sub>)<sub>4</sub> is endothermic. This provides a qualitative explanation for the experimental observation of incomplete ammonolysis of titanium tetrachloride. For an accurate estimation of the free energy of ammonolysis, the entropy changes and the solvolysis of reactants and products must be taken into account.

Transition state energies for the ammonolysis reactions of TiCl<sub>4-x</sub>(NH<sub>2</sub>)<sub>x</sub> molecules are shown in Table 7. The corresponding structures are given in Figure 4. We located the transition states at all three levels for the first two reactions, at HF and MP2 for the third reaction, and only at HF for the last step of the ammonolysis. The transition state structures for all steps of the ammonolysis have very long Ti–Cl distances for the leaving Cl atoms (product-like). A comparison of the structures shown in Figure 4 at the HF level shows a clear trend of “shifting” the TS geometries toward the dissociation products with proceeding ammonolysis. This observation explains the increasing difficulty in locating the TS



**Figure 4** B3LYP optimized geometries of transition states during dichlorinations of (a)  $TiCl_4-NH_3$ , (b)  $TiCl_3NH_2-NH_3$ , (c)  $TiCl_2(NH_2)_2-NH_3$ , (d)  $TiCl(NH_2)_3-NH_3$ . HF and MP2 values are given in parentheses

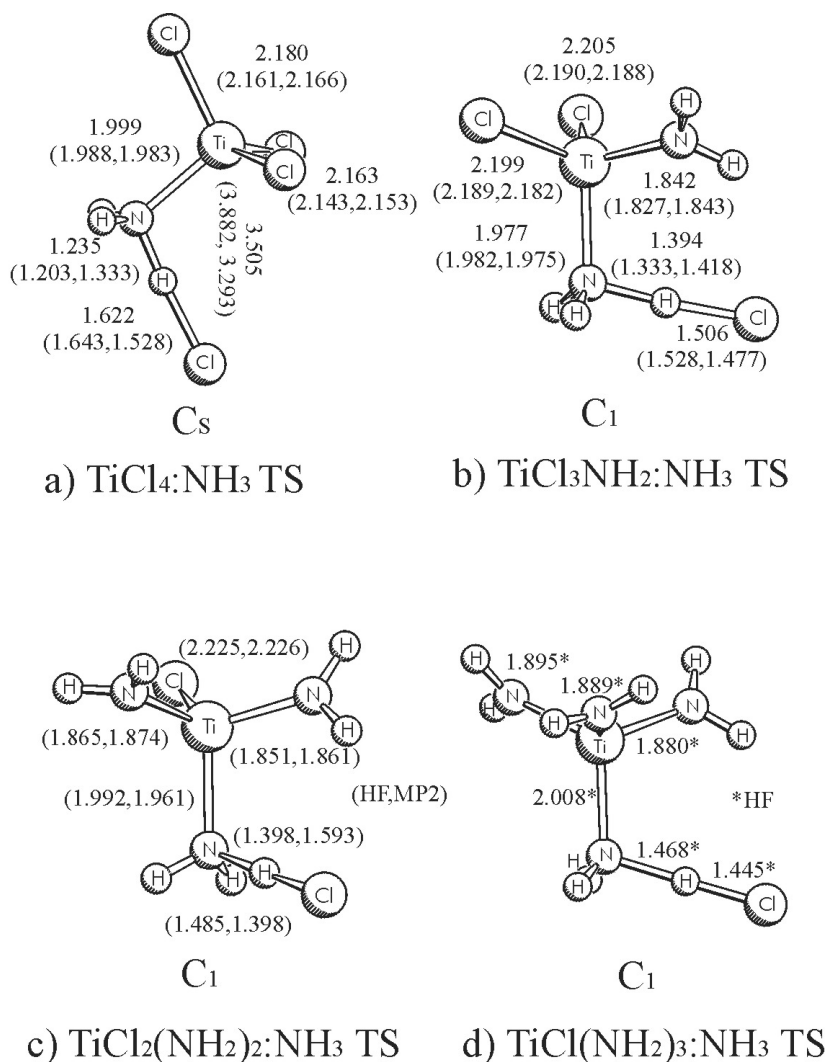


**Figure 5** Calculated reaction path for the formation of  $TiCl_4-NH_3$  complex and further ammonolysis at CCSD(T). Relative energies at HF, MP2 and B3LYP are given in parentheses

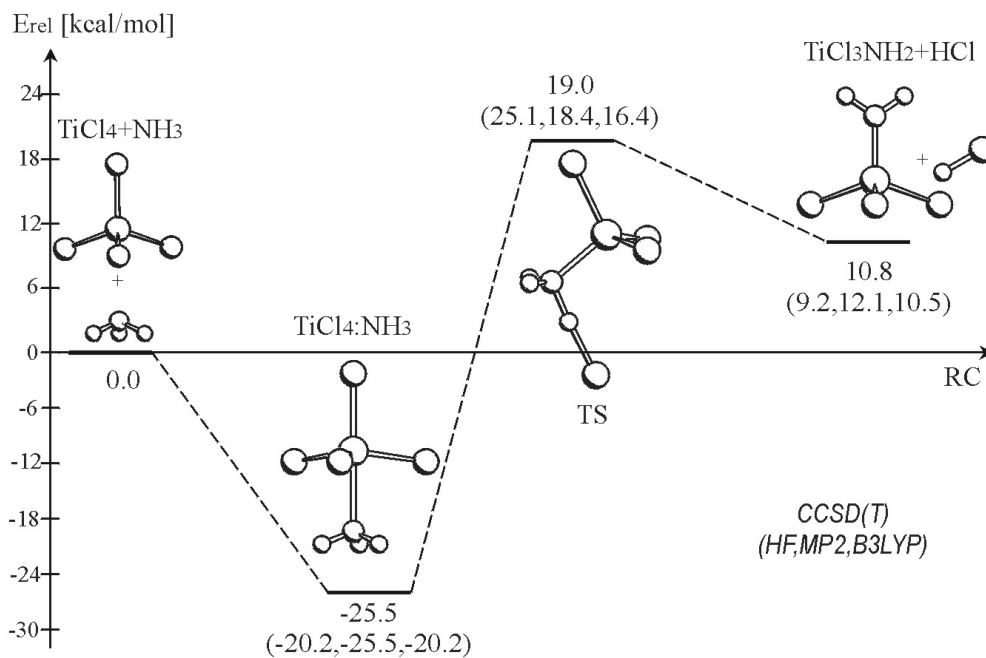


**Table 7** Transition state energies in reactions of substitution of Cl atom by NH<sub>2</sub> group in TiCl<sub>4-x</sub>(NH<sub>2</sub>)<sub>x</sub> (x = 0-3) molecules (in kcal mol<sup>-1</sup>)

Reaction	HF	B3LYP	MP2	CCSD(T)
TiCl <sub>4</sub> + NH <sub>3</sub> → TiCl <sub>3</sub> NH <sub>2</sub> + HCl	25.1	16.4	18.4	19.0 [a] 20.4 [b]
TiCl <sub>3</sub> NH <sub>2</sub> + NH <sub>3</sub> → TiCl <sub>2</sub> (NH <sub>2</sub> ) <sub>2</sub> + HCl	19.3	9.6	11.3	12.7 [a] 13.8 [b]
TiCl <sub>2</sub> (NH <sub>2</sub> ) <sub>2</sub> + NH <sub>3</sub> → TiCl(NH <sub>2</sub> ) <sub>3</sub> + HCl	19.0	—	11.0	13.3 [b]
TiCl(NH <sub>2</sub> ) <sub>3</sub> + NH <sub>3</sub> → Ti(NH <sub>2</sub> ) <sub>4</sub> + HCl	19.9	—	—	15.5 [b]

[a] at CCSD(T)//B3LYP

[b] at CCSD(T)//HF

structures at correlated levels, which usually have lower barriers and thus flatter potential energy surfaces in the barrier region. Since the B3LYP optimized geometries have not been located, we used the HF optimized geometries for computation of the single point CCSD(T) energies of the transition states for the last two reactions in Table 7. To validate their comparison with other CCSD(T) energies computed at the B3LYP optimized geometries, we calculated both CCSD(T)/B3LYP and CCSD(T)/HF energies for the transition states in the first two reactions in Table 6. Although the N··H and H··Cl distances vary substantially in different approaches for the first two TS structures shown in Figure 4, CCSD(T) energies computed at HF and B3LYP differ only by ~1 kcal mol<sup>-1</sup>. This comparison confirms the flat character of the potential energy surface in the barrier region. It also validates comparison of the CCSD(T)/HF energies for transition states with the CCSD(T)/B3LYP energies calculated for molecules and complexes.

The TS for the first step of ammonolysis of TiCl<sub>4</sub> has appreciably higher energy, than subsequent substitution of Cl by NH<sub>2</sub>. Only for the first reaction step between TiCl<sub>4</sub> and NH<sub>3</sub> and for the second one at the HF level the energies of the transition states are above the product energies (see energy diagram in Figure 5 and compare the energies in Tables 5 and 6). For the following Cl substitution by the NH<sub>2</sub> groups, the transition state energies are below the product energies,

which shows that (weak) hydrogen bonded complexes exist as intermediates between the transition states and the products. A similar situation has been revealed in our previous study of TaCl<sub>5</sub> hydrolysis in the context of Ta<sub>2</sub>O<sub>5</sub> CVD.[35]

For 1:2 complexes, TS structures were located at all three levels only for the first reactions and at the HF level for the second and third reactions. For the last step of ammonolysis we were not able to locate the TS even at the HF level. Similar to the reactions of four-coordinated molecules with ammonia 1:2 complexes have very loose product-like TS structures for substitution of Cl by NH<sub>2</sub> (Figure 6). The computed TS energies for reactions of the 1:2 complexes with ammonia show (Table 8) similar trends as the corresponding analogs in Table 7. Thus, only the first reaction in Table 8 (see also energy diagram on Figure 7) has a barrier height larger than the energy of the reaction products and larger than the barriers for two subsequent reactions.

## Conclusions

According to our theoretical studies all four steps of TiCl<sub>4</sub> ammonolysis are *endothermic* with the heat of reaction increasing along the pathway of the ammonolysis. In excess of ammonia *exothermic* formation of TiCl<sub>4-x</sub>(NH<sub>2</sub>)<sub>x</sub> provides the

**Figure 6** B3LYP optimized geometries of transition states during dichlorinations of (a) TiCl<sub>4</sub>:2NH<sub>3</sub>, (b) TiCl<sub>3</sub>NH<sub>2</sub>:2NH<sub>3</sub>, (c) TiCl<sub>2</sub>(NH<sub>2</sub>)<sub>2</sub>:2NH<sub>3</sub>, (d) TiCl(NH<sub>2</sub>)<sub>3</sub>:2NH<sub>3</sub>. HF and MP2 values are given in parentheses

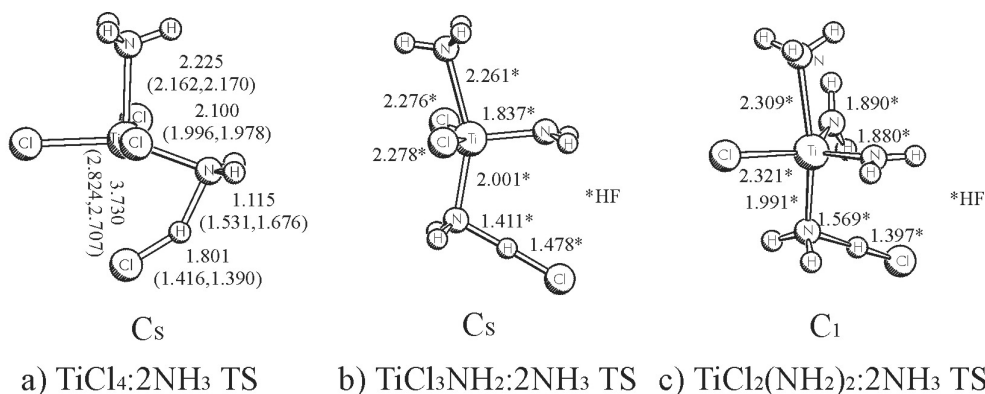


**Table 8** Transition state energies in reactions of substitution of Cl atom by NH<sub>2</sub> group in TiCl<sub>4-x</sub>(NH<sub>2</sub>)<sub>x</sub>:NH<sub>3</sub> (x = 0-3) complexes (in kcal mol<sup>-1</sup>)

Reaction	HF	B3LYP	MP2	CCSD(T)
TiCl <sub>4</sub> :NH <sub>3</sub> + NH <sub>3</sub> → TiCl <sub>3</sub> NH <sub>2</sub> :NH <sub>3</sub> + HCl	31.4	15.7	21.2	18.6 [a] 22.0 [b]
TiCl <sub>3</sub> NH <sub>2</sub> :NH <sub>3</sub> + NH <sub>3</sub> → TiCl <sub>2</sub> (NH <sub>2</sub> ) <sub>2</sub> :NH <sub>3</sub> + HCl	17.8	—	—	14.3 [b]
TiCl <sub>2</sub> (NH <sub>2</sub> ) <sub>2</sub> :NH <sub>3</sub> + NH <sub>3</sub> → TiCl(NH <sub>2</sub> ) <sub>3</sub> :NH <sub>3</sub> + HCl	18.3	—	—	14.6 [b]
TiCl(NH <sub>2</sub> ) <sub>3</sub> :NH <sub>3</sub> + NH <sub>3</sub> → Ti(NH <sub>2</sub> ) <sub>4</sub> :NH <sub>3</sub> + HCl	—	—	—	—

[a] at CCSD(T)//B3LYP

[b] at CCSD(T)//HF

thermodynamic driving force for ammonolysis. Our estimation shows that the first three steps of ammonolysis are exothermic in excess of ammonia, while the last one is endothermic, in agreement with an experimental observation of incomplete substitution of Cl atoms by NH<sub>2</sub> groups in gaseous and liquid ammonia.

The transition state structures for substitution of Cl atoms by NH<sub>2</sub> are close to the reaction products. For all but the first step of the ammonolysis, the transition states have energies below those of the separated reaction products because of H-bond formation between nitrogen and HCl. The transition states structures “shift” further toward the products with an increasing number of NH<sub>2</sub> group in the reactant. This complicates their locations on the flat potential energy surface particularly for correlated methods, MP2 and B3LYP. The optimized geometries at B3LYP, HF and MP2 are generally in good agreement with each other. All three correlated methods MP2, B3LYP and CCSD(T) give similar values for reac-

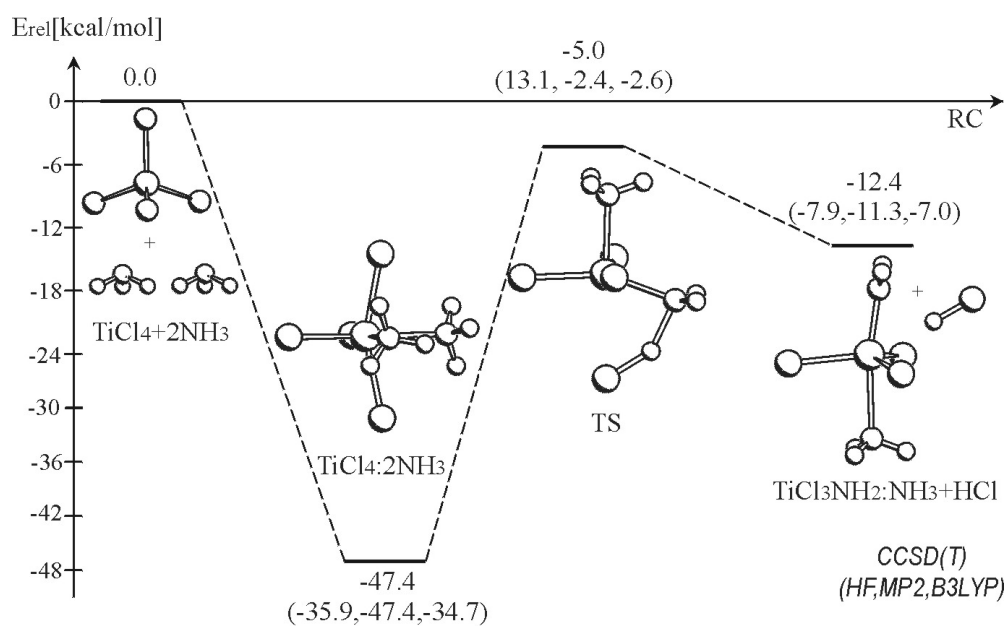
tion energies, while B3LYP underestimates the complex formation energies compared to the other two methods.

**Acknowledgement** This work was supported by the Deutsche Forschungsgemeinschaft (Graduiertenkolleg Metallorganische Chemie) and Alexander von Humboldt Foundation (Fellowship to AK). We acknowledge excellent service and generous allotment of computer time of the Computational Technology Lab at Semiconductor Products Sector, Motorola, HRZ Marburg and HHLRZ Darmstadt. We would also like to thank Dr. Ted Mihopoulos for useful discussion.

## References and notes

- Hoffman, D. M. *Polyhedron* **1994**, *13*, 1169.
- (a) Nicolet, M.-A. *Thin Solid Films* **1978**, *52*, 415. (b) Wittmer, M.; Studer, B.; Melchior, H. *J. Appl. Phys.* **1981**,

**Figure 7** Calculated reaction path the formation of TiCl<sub>4</sub>-2NH<sub>3</sub> complex and further ammonolysis reaction at CCSD(T). Relative energies at HF, MP2 and B3LYP are given in parentheses



- 52, 5722. (c) Anamori, S. *Thin Solid Films* **1986**, *136*, 195. (d) Park, K.C.; Kim, K. B. *J. Electrochem. Soc.* **1995**, *142*, 3109.
3. Kurtz, S. R.; Gordon, R. G. *Thin Solid Films* **1986**, *140*, 277.
4. Raaijmakers, I. J. *Thin Solid Films* **1994**, *247*, 85.
5. (a) Dubois, L. H.; Zegarski, B. R. *J. Electrochem. Soc.* **1992**, *139*, 3603. (b) Prybyla, J. A.; Chiang, C.-M.; Dubois, L. H. *J. Electrochem. Soc.* **1993**, *140*, 2695. (c) Weiller, B. H. *J. Am. Chem. Soc.* **1996**, *118*, 4975.
6. Musher, J. N.; Gordon, R. G. *J. Electrochem. Soc.* **1996**, *143*, 736.
7. Lee, J. G.; Choi, J. H.; Lee, C.; Hong, J. H., Lee, E. G. *Jpn. J. Appl. Phys.* **1998**, *37*, 6942.
8. (a) Fowles, G. W. A. In *Progress in Inorganic Chemistry*; Cotton, F.A., Ed.; Interscience Publishers: New York, 1964; Vol 6, p 1. (b) Clark, R. J. H. In *Comprehensive Inorganic Chemistry*; Bailor, J. C., Jr.; Emeleus, H. J.; Nyholm, R., Trotman-Dickenson, A. F., Eds.; Pergamon Press: Oxford, 1973; Vol 3., p.355.
9. Saeki, Y.; Matsuzaki, R.; Yajima, A.; Akiyama, M. *Bull Chem. Soc. Jpn.* **1982**, *55*, 3193.
10. Allendorf, M. D.; Janssen, C. L.; Colvin, M. E.; Melius, C. F.; Niesen, I. M. B.; Osterheld, T. H.; Ho, P. *Electrochem. Soc. Proc.* **1995**, *95-4*, 393.
11. Baboul, A.G., Schelegel, H.B. *J. Phys. Chem. B*, **1998**, *102*, 5152.
12. (a) Møller, C.; Plesset, M. S. *Phys. Rev.* **1934**, *46*, 618. (b) Binkley, J. S.; Pople, J. A. *Int. J. Quantum Chem.* **1975**, *9S*, 229.
13. Becke, A. D. *J. Chem. Phys.* **1993**, *98*, 5648.
14. Gaussian98 Revision A.3; Frisch, M. J.; Trucks, G. W.; Schlegel, H. B.; Secures, G. E.; Robb, M. A.; Cheeseman, J. R.; Zakrzewski, V. G.; Montgomery, J. A., Jr.; Stratmann, R. E.; Burant, J. C.; Dapprich, S.; Millam, J. M.; Daniels, A. D.; Kudin, K. N.; Strain, M. C.; Farkas, O.; Tomasi, J.; Barone, V.; Cossi, M.; Cammi, R.; Mennucci, B.; Pomelli, C.; Adamo, C.; Clifford, S.; Ochterski, J.; Petersson, G. A.; Ayala, P. Y.; Cui, Q.; Morokuma, K.; Malick, D. K.; Rabuck, A. D.; Raghavachari, K.; Foresman, J. B.; Cioslowski, J.; Ortiz, J. V.; Stefanov, B. B.; Liu, G.; Liashenko, A.; Piskorz, P.; Komaromi, I.; Gomperts, R.; Martin, R. L.; Fox, D. J.; Keith, T.; Al-Laham, M. A.; Peng, C. Y.; Nanayakkara, A.; Gonzalez, C.; Challacombe, M.; Gill, P. M. W.; Johnson, B.; Chen, W.; Wong, M. W.; Andres, J. L.; Gonzalez, C.; Head-Gordon, M.; Replogle, E. S.; Pople, J. A. Gaussian, Inc., Pittsburgh PA, 1998.
15. Hehre, W. J.; Radom, L.; Pople, J. A.; Schleyer, P. v. R. *Ab Initio Molecular Orbital Theory*; Wiley & Sons: New York, 1986.
16. (a) Cizek, J. *J. Chem. Phys.* **1966**, *45*, 4256. (b) Pople, J. A.; Krishnan, R.; Schlegel, H. B.; Binkley, J. S. *Int. J. Quantum Chem.* **1978**, *14*, 545. (c) Bartlett, R. J.; Purvis, G. D. *Int. J. Quantum Chem.* **1978**, *14*, 561. (d) Purvis, G. D.; Bartlett, R. J. *J. Chem. Phys.* **1982**, *76*, 1910. (e) Raghavachari, K.; Trucks, G. W.; Pople, J. A.; Head-Gordon, M. *Chem. Phys. Lett.* **1989**, *157*, 479. (f) Bartlett, R. J.; Watts, J. D.; Kucharski, S. A.; Noga, J. *Chem. Phys. Lett.* **1990**, *165*, 513.
17. For some reactions we were unable to locate transition state structures at the correlated level. In these cases CCSD(T) single calculations were carried out on the HF optimized geometries.
18. Frenking, G.; Antes, I.; Böhme, M.; Dapprich, S.; Ehlers, A. W.; Jonas, V.; Neuhaus, A.; Otto, M.; Stegmann, R.; Veldkamp, A.; Vyboischchikov, S. F. In *Reviews in Computational Chemistry*; Lipkowitz, K. B.; Boyd, D. B., Eds.; VCH Publishers: New York, 1996, Vol 8, p 63.
19. Hay, P. J.; Wadt, W. R. *J. Chem. Phys.* **1985**, *82*, 299.
20. Bergner, A.; Dolg, M.; Kuechle, W.; Stoll, H.; Preuss, H. *Mol. Phys.* **1993**, *80*, 1413.
21. Huzinaga, S. *Gaussian basis sets for molecular calculations*; Elsevier Science: New York, 1984.
22. Russo, T. V.; Martin, R. L.; Hay, P. J. *J. Phys. Chem.* **1995**, *99*, 17085.
23. (a) Ditchfield, R.; Hehre, W. J.; Pople, J. A. *J. Chem. Phys.* **1971**, *54*, 724. (b) Hariharan, P. C.; Pople, J. A. *Theor. Chim. Acta* **1973**, *28*, 213. (c) Francl, M. M.; Pietro, W. J.; Hehre, W. J.; Binkley, J. S.; Gordon, M. S.; DeFrees, D. J.; Pople, J. A. *J. Chem. Phys.* **1982**, *77*, 3654.
24. Cotton, F. A.; Wilkinson, G. *Advanced Inorganic Chemistry*, 4th ed.; Wiley & Sons: New York, 1980; p. 700.
25. Fowles, G. W. A.; Pollard, F. H. *J. Chem. Soc.* **1953**, 527, 2588.
26. Kurtz, S. R.; Gordon, R. G.; *Thin Solid Films* **1986**, *140*, 277.
27. Morino, Y.; Uehara, H. *J. Chem. Phys.* **1966**, *45*, 4543.
28. Jonas, V.; Frenking, G.; Reetz, M. T., *J. Comput. Chem.* **1992**, *13*, 919.
29. Krömer, R.; Thiel, W. *Chem. Phys. Lett.* **1992**, *189*, 105.
30. Sosa, C.; Andzelm, J.; Elkin, B. C.; Wimmer, E.; Dobbs, K. D.; Dixon, D. A., *J. Phys. Chem.* **1992**, *96*, 6630.
31. Cundari, T. R.; Gordon, M. S. *J. Am. Chem. Soc.* **1993**, *115*, 4210.
32. Haaland, A.; Rypdal, K.; Volden, H. V.; Andersen, R. A. *J. Chem. Soc., Dalton Trans.* **1992**, 891.
33. Lappert, M. F.; Power, P. P.; Sangerand, A. R.; Srivasta, R. C. *Metal and Metalloid Amides*; Ellis Horwood: Chichester, 1980; p 475.
34. Beste, A.; Krämer, O.; Fischer, A.; Frenking, G. *Eur. J. Inorg. Chem.* **1999**, 2037.
35. Although *geometric isomers* may be considered as a more appropriate term for considering bipyramodal structures with different axial-equatorial configurations, we call them *conformations* in this paper, since energy variations for this type of *isomerism* is in a few kcal mol<sup>-1</sup> range.
36. Wells, A. F. *Structural Inorganic Chemistry*; Clarendon Press: Oxford, 1975.
37. Siodmiak, M.; Frenking, G.; Korkin, A. *J. Phys. Chem.* in print.
38. (a) Szczesniak, M. M.; Kurnig, I. J.; Scheiner, S. *J. Chem. Phys.* **1988**, *89*, 3131. (b) Del Bene, J. E. *J. Comput. Chem.* **1989**, *10*, 603. (c) Chiport, C.; Rinaldi, D.; Rivail, J.-L. *Chem. Phys. Lett.* **1992**, *191*, 287.